J. Biochem. **127**, 163–169 (2000)

Identification of Key Residues in Rabbit Liver Microsomal Cytochrome P450 2B4: Importance in Interactions with NADPH-Cytochrome P450 Reductase[1]

Michael Lehnerer,* Johannes Schulze,* Klaus Achterhold,† David F.V. Lewis,‡ and Peter Hlavica*,[2]

**Walther-Straub-Institut für Pharmakologie und Toxikologie der LMU, Nussbaumstrasse 26, D-80336 München, Germany; †Physik-Department E17 der TU München, D-85747 Garching, Germany; and ‡Molecular Toxicology Group, School of Biological Sciences, University of Surrey, Guildford GU2 5XH, UK*

Received September 27, 1999; accepted October 28, 1999

A cytochrome P450 2B4 (CYP2B4) model was used to select key residues supposed to serve in interactions with NADPH-cytochrome P450 reductase (P450R). Eight amino acid residues located on the surface of the hemoprotein were chosen for mutagenesis experiments with CYP2B4(Δ2-27) lacking the NH_2-terminal signal anchor sequence. The mutated proteins were expressed in *Escherichia coli*, purified, and characterized by EPR- and CD-spectral analysis. Replacement of histidine 226 with alanine caused a 3.8-fold fall in the affinity for P450R with undisturbed reductive capacity of the system. Similarly, the K225A, R232A, and R253A variants exhibited P450R-directed activity that was depressed to about half that of the control enzyme, suggesting that the deletion of positive charges on the surface of CYP2B4(Δ2-27) resulted in impaired electrostatic contacts with complementary amino acids on the P450R protein. While the Y235A mutant did not show appreciably perturbed reduction activity, the conservative substitution with alanine of the phenylalanine residues at positions 223 and 227 gave a 2.1- to 6.1-fold increase in the K_m values with unchanged V_{max}; this was attributed to the disruption of hydrophobic forces rather than to global structural rearrangement(s) of the engineered pigments. Measurement of the stoichiometry of aerobic NADPH consumption and H_2O_2 formation revealed the oxyferrous forms of the F223A, H226A, and F227A mutants to autoxidize more readily owing to less efficient coupling of the systems. Noteworthy, the F244A enzyme did not exhibit significant reduction activity, suggesting a pivotal role of Phe-244 in the functional coupling of P450R. The residue was predicted to constitute part of an obligatory electron transfer conduit through π-stacking with Phe-296 located close to the heme unit. All of the residues examined reside in the putative G helix of CYP2B4, so that this domain obviously defines part of the binding site for P450R.

Key words: cytochrome P450 2B4, reductase binding, surface residues.

Cytochrome P450 (P450 or CYP) enzymes, a superfamily of hemoproteins, are major catalysts participating in the monooxygenation of a diversity of exo- and endobiotic compounds (*1*). The versatility of these oxygenases has created a great deal of interest in understanding their structure and function. NADPH-P450 oxidoreductase (P450R), which contains one molecule each of FAD and FMN, and cytochrome b_5 have been recognized to constitute components of the microsomal electron-transport chain (*2, 3*). While P450R can donate both the first and second electron to various microsomal P450s, cytochrome b_5 can only transfer the second electron to the oxyferrous hemoproteins owing to its specific redox properties (*4*). The problem of donor/acceptor recognition has been the most important and intriguing one in the area of P450 research. The involvement of both electrostatic and hydrophobic forces in protein–protein interactions has been demonstrated (*5–9*). The availability of crystal structures for some bacterial P450s (*10, 11*), P450R (*12*), and cytochrome b_5 (*13*) has stimulated studies on the molecular modelling of electron-transfer complexes generated with certain P450s and their donor proteins (*14, 15*). Nevertheless, the questions of where and how P450s may interact with their redox partners and what the precise nature of the mechanisms serving in the transfer of reducing equivalents remain to be answered.

Based on a three-dimensional CYP2B4 model, binding sites for P450R and cytochrome b_5 predicted to be located in the C and C° helices have recently been confirmed using genetically engineered CYP2B4 variants (*16*). The present paper draws attention to the role in interactions with

[1] This work was supported by grant HI 1/15-1 from the Deutsche Forschungsgemeinschaft (M.L., J.S., and P.H.) and funds from GlaxoWellcome Research and Development Ltd, Merck Sharp & Dohme Ltd, The European Union and The University of Surrey (D.F.V.L.).

[2] To whom correspondence should be addressed. Phone: +49 89 5160-7219, Fax: +49 89 5160-7207, E-mail: Hlavica@lrz.uni-muenchen.de

Abbreviations: P450 or CYP, cytochrome P450 [EC 1.14.14.1]; P450R, NADPH-cytochrome P450 oxido-reductase [EC 1.6.2.4]; SDS-PAGE, sodium dodecylsulfate-polyacrylamide gel electrophoresis.

P450R of charged and aromatic amino acid residues residing in the putative G helix of CYP2B4.

MATERIALS AND METHODS

Materials—NADPH, glucose 6-phosphate, glucose 6-phosphate dehydrogenase [EC 1.1.1.49], glucose oxidase [EC 1.1.3.4], and catalase [EC 1.11.1.6] were obtained from Roche Diagnostics (Mannheim, Germany). Dilauroyl L-α-phosphatidylcholine and hexobarbital were purchased from Sigma (Deisenhofen, Germany). All other reagents were of the highest purity commercially available.

Protein Expression and Purification—The vector pGEX-KT-2B4(Δ2-27), serving to express recombinant CYP2B4 lacking amino acid residues 2–27, was generously provided by Dr. Minor J. Coon (University of Michigan, Ann Arbor, MI). The CYP2B4 (Δ2-27) cDNA of the construct was found to encode for Ser at position 221 of the polypeptide. Noteworthy, data from protein sequencing indicate either Ser (*17*) or Pro (*18*) at this position. Oligonucleotide-directed mutation of the truncated CYP2B4 giving rise to an exchange of Pro for Ser-221 has been recently reported to produce a catalytically competent enzyme, as tested in a typical reaction with benzphetamine as substrate in the presence of either P450R (*19*) or cumene hydroperoxide in place of the reductase (*20*).

The pairs of sense and anti-sense primers designed to generate CYP2B4 (Δ2-27) variants were chemically synthesized by Eurogentec (Heidelberg, Germany) and are listed in Table I. Mutations were introduced using the Quik Change™ protocol (*21*). Briefly, standard PCR amplification was carried out for 16 cycles in reaction mixtures containing 200 μM dNTPs, 1.5 mM $MgCl_2$, 1 μM primers, 100 ng of template DNA, and 1 U of *Pfu* DNA polymerase (Eurogentec, Heidelberg, Germany) in PCR buffer (Stratagene, Heidelberg, Germany). The template DNA was digested with *Dpn*I, and 2 μl of digest were used to transform competent *Escherichia coli* JM109 cells. Transformants carrying DNA encoding for the desired amino acid exchanges were selected using a ^{T7}Sequencing Kit (Pharmacia Biotech, Freiburg, Germany).

The proteins were expressed fused to glutathione *S*-transferase in the *E. coli* host strain to yield 33–260 nmol P450/liter of cell culture. The fusion proteins were liberated from the transferase moiety by thrombin treatment and purified to a specific content of 11.3–14.9 nmol P450/mg protein as described previously (*22*). The concentration of the recombinant pigments was determined as indicated by Omura and Sato (*23*) using a molar absorption coefficient of 91,000 $M^{-1}\cdot cm^{-1}$. The final preparations were subjected to analysis by SDS-PAGE on slab gels containing 12% (m/v) acrylamide (*24*) followed by Western blotting (*25*). Immunoreactive bands were detected by a polyclonal CYP2B4 antibody with peroxidase-conjugated anti-goat immunoglobulin (Sigma, Deisenhofen, Germany) as the secondary antibody. Protein was measured by the Lowry procedure (*26*).

P450R, isolated from hepatic microsomes of male New Zealand White rabbits as reported elsewhere (*27*), exhibited a specific activity of 40 μmol of cytochrome *c* reduced/min per mg protein. The flavoprotein was quantified by its absorbance at 456 nm using a molar absorption coefficient of 21,400 $M^{-1}\cdot cm^{-1}$ (*28*).

Spectral Measurements—Electronic absorption spectra of the proteins were recorded at room temperature with a Shimadzu UV1601PC spectrophotometer; optical pathlength was 1.0 cm.

EPR measurements were carried out at 20 K with a Bruker Elexsys 500 spectrometer. Typical spectrometer settings were: microwave power, 10 mW; modulation amplitude, 3 mT; frequency, 9.47 GHz; sweep time, 42 s; sweep width, 125 mT; time constant, 1.28 ms. The data from ten scans were averaged. The samples contained 15 μM P450 in 100 mM sodium phosphate buffer (pH 7.4) containing 20% (v/v) glycerol.

CD spectra in the far ultraviolet and visible regions were monitored at room temperature with a Jasco J-715 spectropolarimeter; the optical pathlengths were 0.1 and 1.0 cm, respectively. Measurements were conducted in 50 mM sodium phosphate (pH 7.4) containing 0.5 to 5 μM P450. The standard conditions were as follows: band width, 1 nm; response, 1–2 s; step resolution, 0.1–0.2 nm. Blanks (buffer without hemoprotein) were routinely recorded and substracted from the original spectra. On average, data from 5–10 scans were accumulated.

Enzyme Assays—The NADPH-supported reduction of ferric P450 was measured at 25°C in reaction mixtures composed of 2 μM P450, varying amounts of P450R, 48 μM dilauroyl phosphatidylcholine (sonicated until clarification was observed), 1 mM hexobarbital, 100 mM glucose, glucose oxidase (400 μg/ml), and catalase (75 μg/ml) in 100 mM sodium phosphate buffer (pH 7.4) containing 20% (v/v) glycerol. The system was preincubated at room temperature for 15 min to allow efficient association of the redox proteins in the micellar matrix. Subsequently, the samples were gassed for 5 min with CO. Reactions were initiated by the rapid addition of NADPH to yield a final concentration of 1 mM using a set of plunger cuvettes. Absorbance changes at 450 nm were recorded with a Shimadzu UV 1601PC spectrophotometer. Apparent K_m and V_{max} values were calculated from a non-linear least squares fit of the initial velocity data to the Michaelis-Menten kinetics (*29*) using Corel QuattroPro 7.0 software.

In some studies, the rates of reduction were assessed in systems in which ferric P450 and P450R did not exist in the preformed complex described above. In this case, 4 μM P450 and 0.2 μM P450R were separately combined in two syringes with 48 μM phospholipid dissolved in 100 mM phosphate buffer (pH 7.4) in the presence of 1 mM hexobarbital, 1 mM NADPH, and a deoxygenating system. The samples were incubated at 25°C for 15 min. After gentle bubbling of the mixtures with CO, the syringes were transferred to an Aminco Dasar/DW-2 spectrophotometer equipped with an Aminco-Morrow stopped-flow apparatus; dead time of the instrument was 4 ms. The extent of P450 reduction was determined by monitoring the formation of the carbonyl adduct at 450 nm upon rapid mixing of the contents of the two syringes.

NADPH oxidase activity was measured at 25°C in aerobic media comprising 2 μM P450, 0.5 μM P450R, 48 μM dilauroyl phosphatidylcholine, 2 mM hexobarbital and 50 μM NADPH in 100 mM sodium phosphate buffer (pH 7.4) supplemented with 20% (v/v) glycerol. Disappearance of the reduced cofactor was followed by the decrease in absorbance at 340 nm using a molar absorption coefficient of 6220 $M^{-1}\cdot cm^{-1}$ (*30*). For determining H_2O_2 production, the

above mixtures were fortified with an NADPH-regenerating system consisting of 10 mM glucose 6-phosphate, 6 mM $MgCl_2$, and glucose 6-phosphate dehydrogenase (5 μg/ml) and incubated at room temperature for 20 min. Peroxide was quantified by the ferrithiocyanate method (*31*).

Molecular Modelling—Structure investigations on P450 were carried out according to a recent three-dimensional CYP2B4 model based on multiple protein sequence homology alignment with the substrate-bound CYP102 template. The model was constructed and refined using the Sybyl Biopolymer and Tripos force field protein analysis programs as described previously (*32*).

RESULTS AND DISCUSSION

Spectral Characterization of the Recombinant Proteins—Truncated CYP2B4 and its mutated derivatives were expressed in *E. coli* fused to glutathione *S*-transferase and purified following cleavage of the proteins with thrombin. The pigments did not undergo degradation during the expression and purification processes, as evidenced by immunoblot analysis (data not shown). All the hemoprotein species listed in Table I generated normal CO-reduced difference spectra, with the position of the Soret bands ranging from 451.1 to 451.7 nm. The A_{418}/A_{394} ratios in the electronic absorption spectra of the oxidized enzymes varied from 2.1 to 2.9. These spectral characteristics are comparable to those reported for highly purified rabbit liver microsomal low-spin CYP2B4 (*33*).

In order to recognize the potential effects of amino acid replacement on the structure of the heme site, EPR-spectral measurements were carried out with a number of deletion mutants selected for closer analysis. As shown in Fig. 1, the oxidized forms of both the truncated wild type and engineered congeners exhibited spectra consistent with substrate-free, low spin ferric CYP2B4, with *g* values in the high field region of $g_x=1.92$, $g_y=2.25$, and $g_z=2.43$ (*33*). Moreover, a small signal of variable intensity was observed throughout the spectra characterized by a *g* value of about 2.02; the source of this band remains obscure. In the low field region, a signal at $g=4.28$ appeared in all spectra (data not shown) and was tentatively attributed to the presence of trace amounts of adventitious iron (*33*). While the paramagnetic properties of mutants H226A, F227A, and F244A thus were analogous to those of the wild type, providing evidence of an undisturbed heme assembly, the spectrum of the F223A variant exhibited a splitting of the g_x and g_z bands, possibly reflecting subtle conformational changes in the immediate heme environment.

Further structural information was obtained from CD-spectral measurements. The spectra recorded with the H226A, F227A, and F244A mutant enzymes in the visible region (Fig. 2B) were very similar to CYP2B4 (Δ2-27) in terms of band shape and peak position, disproving a

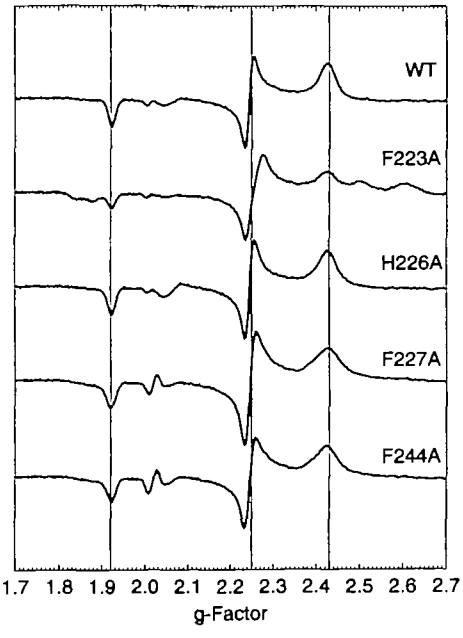

Fig. 1. **EPR spectra of CYP2B4(Δ2-27) and some of its deletion mutants.** Measurements were carried out at 20 K with 15 μM P450 in 100 mM sodium phosphate (pH 7.4) as detailed in "MATERIALS AND METHODS"; WT, truncated wild type.

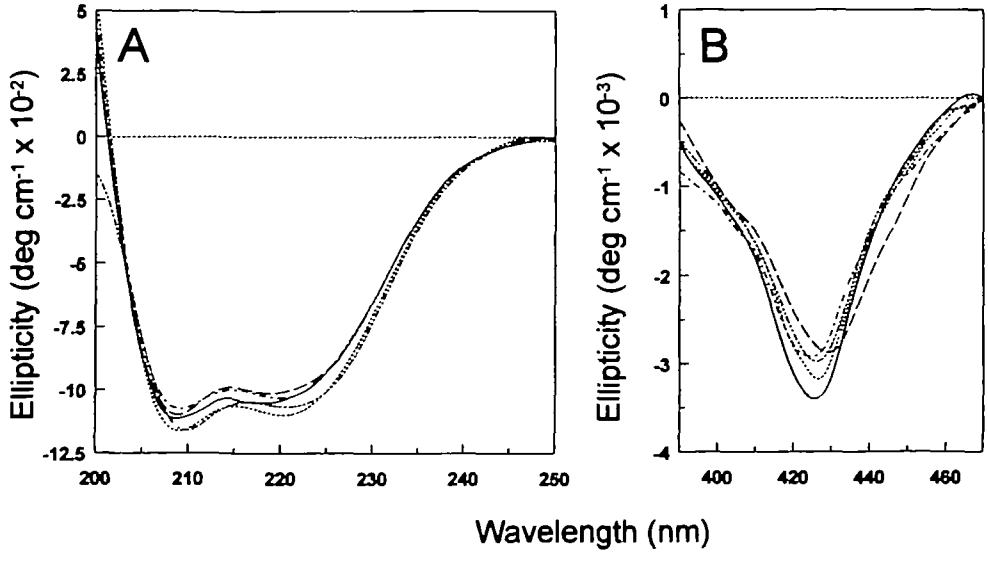

Fig. 2. **CD spectra of CYP2B4 (Δ2-27) and some of its mutated variants.** CD-spectral changes in the far ultraviolet (A) and visible (B) regions were recorded for solutions containing 0.5 to 5 μM P450 in 50 mM sodium phosphate (pH 7.4). The spectra depicted pertain to the truncated wild type (——) and mutants F223A (- - - - -), H226A (···), F227A (— • —), and F244A (— •• —).

grossly perturbed geometry of the heme vicinity. In contrast, a bathochromic shift by 2.4 nm could be observed for the signal generated by the F223A protein, hinting at a slight rearrangement of the heme site. CD-spectral analysis in the far ultraviolet region revealed almost identical spectra for all enzyme forms investigated (Fig. 2A), the optical tracings being corrected for the presence of apohemoprotein on the basis of the A_{418}/A_{278} ratios in the absorption spectra of the individual preparations (*34*). This behaviour suggested that no major alterations in the global polypeptide backbone folding were introduced by the diverse amino acid substitutions.

TABLE I. **Oligonucleotide sequences of the pairs of sense and anti-sense primers used to mutate CYP2B4 (Δ2-27) cDNA.**

Mutant	Sequence (5′ to 3′)*
F223A	CTC TTC TCG GGC **GCC** CTA AAG CAC TTT
	CGT GCC AGG AAA XX(ACT) CTT TAG GAA GCC
K225A	TCG GGC TTC CTA **GCN** CAC TTT CCT GGC
	CGT GCC AGG AAA NGC CTT TAG GAA GCC
H226A	TCG GGC TTC CTA GCN CAC TTT CCT GGC
	CGT GCC AGG AAA **NGC** CTT TAG GAA GCC
F227A	TTC CTA AAG CAC **GCT** CCT GGC ACG CAC
	CCT GTA GAT CTG CGC ATG CGT GCC AGG
R232A	CCT GGC ACG CAT **GCG** CAG ATC TAC AGG
	CCT GTA GAT CTG **CGC** ATG CGT GCC AGG
Y235A	CAC AGG CAG ATC **GCC** AGG AAC CTG CAG
	CG CAC AGG CAG ATA TAC CGC AAC CTG CAG G
F244A	GAG ATC AAC ACT **GCC** ATC GGC CAG AGC
	CAG GGT TGC GCG NGC CTT CTC TAC GCT
R253A	CAG AGC GTA GAG GCN CAC CGC GCA ACC
	GGG GTC CAG GGT TGC **GGC** ATG CTT CTC TAC GCT

*The bases that were altered to introduce the indicated mutation are shown in bold letters.

Characterization of the Ability of Ferric CYP2B4(Δ2-27) and Mutant P450s to Accept Reducing Equivalents from P450R—CYP2B4(Δ2-27) was subjected to site-directed mutagenesis to study the impact of selected amino acid deletions (Table I) on the functional interaction with P450R. The rationale for the construction of the diverse mutants was provided by both a tentative map of P450 functional domains located on the CYP2B4 surface (*35*) and the well-known involvement of basic (*5, 36*) and aromatic (*34*) residues in P450R recognition. All residues were mutated to the most common amino acid, alanine, in order to evaluate the function of the side chains distal to the β-carbon.

Measurements were conducted with the redox proteins reconstituted into phospholipid. The preincubation period was adequate to compensate for the slow anchoring to the matrix the CYP2B4 species lacking the hydrophobic tail portion (*37*), so that the limited availability of lipid-bound P450s could be ruled out to diminish the statistical proba-

TABIE II. **Initial-velocity kinetic constants for the anaerobic, NADPH-dependent reduction of ferric CYP2B4(Δ2-27) and mutant P450s by P450R.** The apparent K_m and V_{max} values, reflecting the hexobarbital-stimulated reactivities and reductive capacities of P450R toward the recombinant hemoproteins, were taken from the double-reciprocal initial-velocity plots presented in Fig. 3A. Calculations were carried out by non-linear regression analysis as detailed in "MATERIALS AND METHODS." The data are the means ± SEM of three experiments.

CYP2B4(Δ2-27) species studied	Cytochrome P450 reduction		
	K_m (μM)	V_{max} (nmol/min)	V_{max}/K_m (ml/min)
Wild type	0.47±0.04	1.09±0.08	2.32±0.18
F223A	1.00±0.11	0.96±0.10	0.96±0.10
H226A	1.79±0.07	1.13±0.05	0.63±0.03
F227A	2.87±0.34	0.95±0.11	0.33±0.04

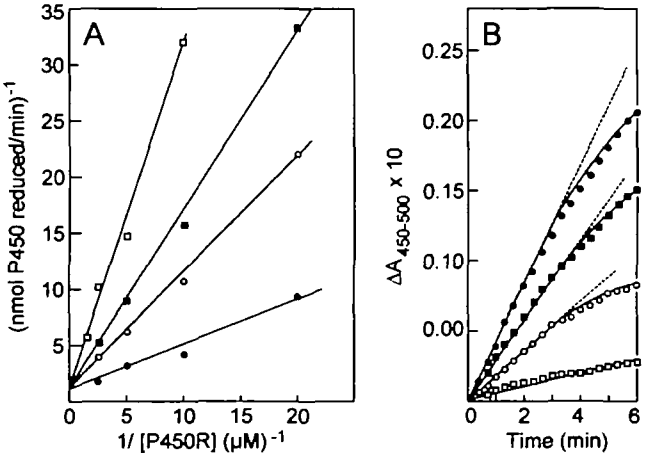

Fig. 3. **NADPH-sustained reduction of ferric CYP2B4(Δ2-27) and some of its mutated derivatives by P450R.** In a first set of experiments (panel A), reactions were started by the addition of NADPH to anaerobic solutions containing P450 protein preincubated with specified amounts of P450R in the presence of hexobarbital; initial rates of electron transfer were fitted to the Michaelis-Menten kinetics by non-linear regression analysis. In a second set of experiments (panel B), NADPH-reduced P450R was rapidly reacted with ferric P450 in the presence of barbiturate to study the time course of association of the redox partners; in this case, the molar ratio of flavo- to hemoprotein was 1:20. The data presented refer to measurements with truncated wild type (●) and the mutants F223A (○), H226A (■), and F227A (□). The points are the means of three experiments.

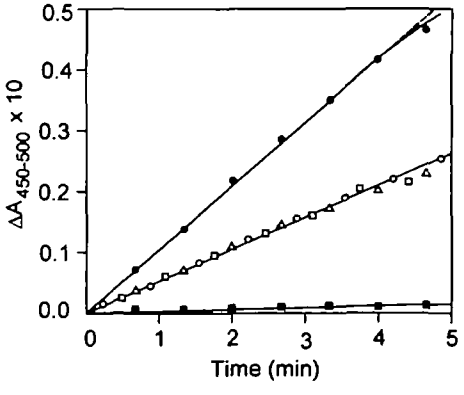

Fig. 4. **Impact of deletion of electrostatic and hydrophobic forces through mutation of CYP2B4(Δ2-27) on electron transfer from P450R.** Rates of NADPH-driven hemoprotein reduction were assessed in reaction mixtures containing 2 μM P450 and 0.1 μM P450R reconstituted into phospholipid in the presence of 1 mM hexobarbital and a deoxygenating system. The data presented refer to analyses with truncated wild type (●) and the mutant proteins K225A (○), R232A (□), R253A (△), and F244A (■). The experimental points are the means of three measurements.

bility of the hemoproteins encountering P450R attached to micellar phospholipid (*38*). Analyses were carried out under strictly anaerobic conditions to avoid autoxidation of the terminal acceptor proteins; the velocities of accumulation of ferrous pigment thus primarily reflect the rates of electron transfer. The kinetic data derived from such assays are plotted in Fig. 3A and are summarized in Table II. As can be seen, there was a 3.8-fold increase in the apparent K_m value for the H226A mutant-reductase complex in the presence of hexobarbital as compared with the truncated wild type, while the V_{max} value was indistinguishable from that for CYP2B4(Δ2-27). From these data, the reductive efficiency (V_{max}/K_m) of the system could be calculated to be 27% that in the CYP2B4(Δ2-27)-dependent route. When the ferric, substrate-bound H226A variant was rapidly mixed with NADPH-reduced P450R, so that association of the redox partners constituted the rate-limiting step in electron transfer, the rate of hemoprotein reduction was found to be 71% that of the wild type-catalyzed reaction (Fig. 3B), suggesting that decreased complex stability rather than impaired association plays a predominant role in the change in affinity for each of the redox components.

The question arose as to what molecular mechanism(s) might be responsible for the defective interaction of the H226A protein with its redox partner. The spectral data presented in Figs. 1 and 2 do not support the notion that substantial structural rearrangement(s) of the hemoprotein compromise the productive coupling of P450R. Instead, deletion of the positive charge at position 226 of the polypeptide might disrupt electrostatic contacts with carboxylate groups on the donor protein. This view is endorsed by the fact that replacement of other positively charged CYP2B4(Δ2-27) residues with alanine to yield the mutants K225A, R232A, and R253A resulted in P450s exhibiting P450R-directed activity decreased to about half that of the wild type (Fig. 4).

Special attention was drawn to the influence of the deletion of aromatic amino acids in CYP2B4(Δ2-27) on the ability of the mutated P450s to accept electrons from P450R. While construction of the Y235A variant affected the hexobarbital-stimulated reductive activity to only a minor extent (data not shown), the conservative exchange of alanine for phenylalanine at positions 223 and 227 gave rise to a 2.1- and 6.1-fold, respectively, increase in the apparent K_m values for reductase binding with undisturbed reductive potencies (V_{max} values). This caused a fall in V_{max}/K_m for the engineered proteins of about 60 to 86%, suggesting that both Phe-223 and Phe-227 play a substantial role in the process of P450R coupling. Inspection of the kinetic tracings presented in Fig. 3B revealed the association of the F223A and F227A mutants with P450R to be decelerated by 57 and 87%, respectively, as compared with the truncated wild type, indicating hampered adduct formation rather than diminished complex stability as the overriding mechanism responsible for the observed increases in the K_m values. Perturbed association of the redox partners was considered to be the consequence of disruption of hydrophobic forces or structural rearrangement(s) at the P450R recognition site(s). As regards the latter possibility, the CD spectra shown in Fig. 2A do not lend much support to the notion of defective protein folding, albeit a slight long-range effect on the geometry of the immediate heme vicinity could not be excluded for the F223A species (*cf.* Figs. 1 and 2B).

Most strikingly, the reduction activity of the F244A construct was too low to permit accurate estimates of the

TABLE III. **Rates of aerobic NADPH consumption and H_2O_2 production by CYP2B4 (Δ2-27) and mutant P450s reconstituted with P450R in the presence of hexobarbital.** Assays were carried out at 25°C in media composed of 2 μM P450, 0.5 μM P450R, 48 μM phospholipid, 2 μM barbiturate, and 50 μM reduced cofactor. NADPH utilization was followed at 340 nm and peroxide-linked formation of ferrithiocyanate was monitored at 480 nm. The data represent the means ± SEM of three experiments.

CYP2B4(Δ2-27) species studied	Activity (nmol/min)		
	NADPH oxidation (a)	H_2O_2 production (b)	(b)/(a)
Wild type	6.09±0.49	1.24±0.33	0.20±0.03
F223A	4.30±0.11	1.27±0.06	0.30±0.01[c]
H226A	3.08±0.12	2.83±0.06	0.92±0.02[c]
F227A	2.80±0.26	1.12±0.02	0.40±0.02[c]

[c]These values differ significantly from the wild-type data with $p < 0.05$ to $p < 0.001$.

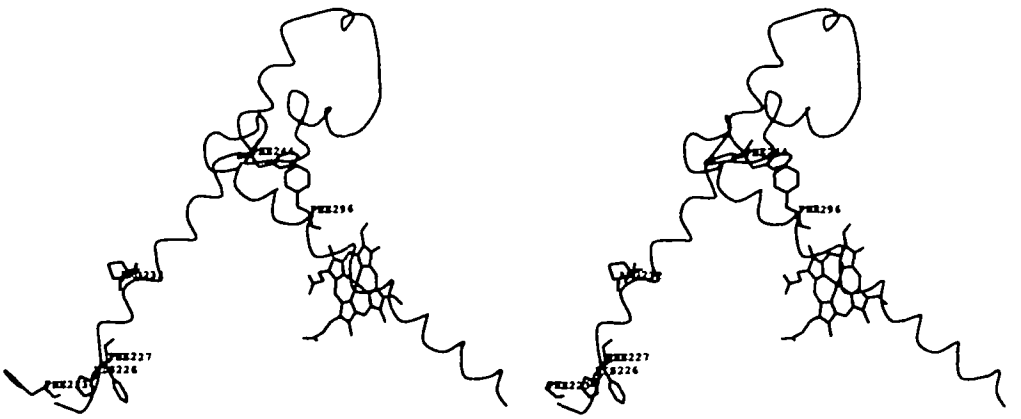

Fig. 5. **Stereodiagram of the topology of residues in the molecular CYP2B4 model participating in interactions with P450R.** The view displays three α-helices (G, H, and I; all in blue) with the side chains of the basic amino acids (in black) and aromatic residues (in green) involved in contacts with P450R coming off the G helix. Also shown is the position in the I helix of Phe-296, π-stacking with Phe-244 and residing in close proximity to the distal heme face (in magenta).

kinetic parameters (Fig. 4). One possible explanation for this finding is that deletion of the Phe-244 side chain alters the critical architecture of the active site in such a way as to modify the interaction with hexobarbital; the latter substrate is known to stimulate reduction activity by inducing a low-to-high spin transition of CYP2B4(Δ2-27) (*39*). However, the spectral analyses summarized in Figs. 1 and 2B, representing sensitive tools for probing the active site of P450s, do not strengthen this concept, as the mutated enzyme did not display appreciable structural anomalies as compared with the control. Alternatively, data obtained with a computer-aided three-dimensional CYP2B4 model (*32*) prompted us to suggest that Phe-244 might be essential to the functional coupling of P450R: the residue was predicted to enter into a π-π stacking interaction with Phe-296, the centres of the aromatic rings being 4.8 Å apart from each other; the latter amino acid was recognized to be located in the putative I helix, which leads directly to the distal face of the porphyrin macrocycle (Fig. 5). This led us to hypothesize that phenylalanines 244 and 296 might constitute part of an obligatory conduit for electron transfer to the heme unit, linking of the aromatic stacking with the prosthetic group occurring *via* the I-helical hydrogen-bonded network. Here, the highly conserved Gly-299 (*40*) appears to be a likely candidate for bridging reducing equivalents to the terminal acceptor: the residue is only 6.5 Å away from the heme iron, satisfying the criteria for thermally activated electron tunneling (*41*). The invariant Thr-302, located at a distance of 5.1 Å from the heme, can be dismissed as a participant in this process, since replacement of threonine with alanine has been previously demonstrated to leave electron flow from P450R to the mutated CYP2B4 (Δ2-27) unaffected (*42*). Clearly, more work is needed to substantiate our hypothesis.

Stoichiometry of NADPH Consumption and Hydrogen Peroxide Formation with CYP2B4 (Δ2-27) and Mutant P450s Reconstituted with P450R under Aerobic Conditions—To further characterize the effect of mutagenesis of CYP2B4(Δ2-27) on electron transfer, NADPH oxidation was measured along with hydrogen peroxide production in aerobic media containing P450/P450R, micellar phospholipid, and hexobarbital as a substrate. In such systems, NADPH oxidase activity has been shown to be almost entirely due to CYP2B4-dependent catalysis rather than cofactor disposal by the P450R component (*43*). In order to assess turnover with a physiologically relevant protein stoichiometry, assays were carried out at a P450R-to-P450 molar ratio far below that routinely used (*43*).

As shown in Table III, the engineered proteins consistently catalyzed NADPH consumption at a decreased rate as compared with CYP2B4(Δ2-27). While H_2O_2 production by the F223A and F227A mutants was regarded as equivalent to that by the truncated wild type, excluding the possibility that amino acid substitution might have destabilized the appropriate iron-hydroperoxo intermediates to release peroxide, the H226A variant gave a 2.3-fold increase in the yield of H_2O_2. Generally, the proportion of peroxide formed to NADPH utilized with barbiturate present was significantly higher for the mutated pigments as compared with the control enzyme. This was interpreted to mean that the amino acid deletions caused the oxyferrous mutant proteins to autoxidize more readily owing to less efficient coupling of the systems. Based on this hypothesis, comparison of the data summarized in Tables I and II suggest that the apparent efficiency of transfer of the second electron to the F223A and F227A species is diminished to a markedly lower extent as compared with that of transfer of the first electron. In contrast, with the H226A polypeptide, the efficacy of both events was depressed almost equally relative to the truncated wild type. This discrepancy could be reconciled by assuming that the small conformational change related to the shift from substrate-bound, ferric high-spin P450 to the oxyferrous low-spin form was beneficial to the functional association with P450R of the former two hemoprotein variants, but was obviously inadequate to partially compensate for the strong decrease in stability of the complex generated with the H226A enzyme and reductase (see above).

Collectively, the studies reported herein enabled us to verify the importance of electrostatic and hydrophobic forces in the recognition of truncated CYP2B4 by P450R, using site-directed mutagenesis to modify basic and aromatic amino acids on the surface of the hemoprotein. It has to be emphasized that all the residues studied are located in the putative G helix of the polypeptide (Fig. 5), which has recently been shown also to accomodate structural elements serving in the proper assembly of CYP2B4 (*39*). The domain obviously defines part of the P450R binding site. The latter has been conclusively demonstrated to also comprise residues located in the C/C* helices (*16*) and a known point of interaction residing in the $\beta_2(2)$-$\beta_1(3)$ turn of CYP2B4 (*44*). Further work is underway to gain a more thorough understanding of the regulation and mechanism of electron transfer, a key step in the P450 catalytic cycle.

The authors thank Elisabeth Weyher (Max-Planck-Institut für Biochemie, Martinsried) for her help in the CD-spectral analyses. We are also indebted to Cortina Keiling for expert technical assistance.

REFERENCES

1. Porter, T.D. and Coon, M.J. (1991) Cytochrome P450. Multiplicity of isoforms, substrates, and catalytic and regulatory mechanisms. *J. Biol. Chem.* **266**, 13469–13472
2. Lu, A.Y.H. and Coon, M.J. (1968) Role of hemoprotein P-450 in fatty acid ω-hydroxylation in a soluble system from liver microsomes. *J. Biol. Chem.* **243**, 1331–1332
3. Morgan, E.T. and Coon, M.J. (1984) Effects of cytochrome b_5 on cytochrome P-450-catalyzed reactions. Studies with manganese-substituted cytochrome b_5. *Drug Metab. Dispos.* **12**, 358–364
4. Noshiro, M., Ullrich, V., and Omura, T. (1981) Cytochrome b_5 as electron donor for oxy-cytochrome P-450. *Eur. J. Biochem.* **116**, 521–526
5. Bernhardt, R., Kraft, R., Otto, A., and Ruckpaul, K. (1988) Electrostatic interactions between cytochrome P-450 and NADPH-cytochrome P-450 reductase. *Biomed. Biochim. Acta* **47**, 581–592
6. Shen, S. and Strobel, H.W. (1992) The role of cytochrome P450 lysine residues in the interaction of cytochrome P450IA1 and NADPH-cytochrome P450 reductase. *Arch. Biochem. Biophys.* **294**, 83–90
7. Tamburini, P.P., White, R.E., and Schenkman, J.B. (1985) Chemical characterization of protein-protein interactions between cytochrome P-450 and cytochrome b_5. *J. Biol. Chem.* **260**, 4007–4015
8. Black, S.D., French, J.S., Williams, C.H., and Coon, M.J. (1979) Role of a hydrophobic peptide in the N-terminal region of NADPH-cytochrome P-450 reductase in complex formation with P-450LM. *Biochem. Biophys. Res. Commun.* **91**, 1528–

1535
9. Lee-Robichaud, P., Kaderbhai, M.A., Kaderbhai, N., Wright, J.N., and Akhtar, M. (1997) Interaction of human CYP17 (P-$450_{17\alpha}$, 17α-hydroxylase-17,20-lyase) with cytochrome b_5: importance of the orientation of the hydrophobic domain of cytochrome b_5. *Biochem. J.* **321**, 857–863
10. Poulos, T.L., Finzel, B.C., and Howard, A.J. (1987) High-resolution crystal structure of cytochrome $P450_{cam}$. *J. Mol. Biol.* **195**, 687–700
11. Ravichandran, K.G., Boddupalli, S.S., Hasemann, C.A., Peterson, J.A., and Deisenhofer, J. (1993) Crystal structure of hemoprotein domain of P450BM-3, a prototype for microsomal P450s. *Science* **261**, 731–736
12. Wang, M., Roberts, D.L., Paschke, R., Shea, T.M., Masters, B.S.S., and Kim, J.J.P. (1997) Three-dimensional structure of NADPH-cytochrome P450 reductase: prototype for FMN- and FAD-containing enzymes. *Proc. Natl. Acad. Sci. USA* **94**, 8411–8416
13. Durley, R.C.E. and Mathews, F.S. (1996) Refinement and structural analysis of bovine cytochrome b_5 at 1.5 Å resolution. *Acta Cryst.* **D52**, 65–76
14. Lewis, D.F.V. (1996) *Cytochrome P450. Structure, Function and Mechanism*, Taylor & Francis, London
15. Lewis, D.F.V., Lake, B.G., Dickins, M., Eddershaw, P.J., Tarbit, M.H., and Goldfarb, P.S. (1999) Molecular modelling of CYP2B6, the human CYP2B isoform, by homology with the substrate-bound CYP102 crystal structure: evaluation of CYP2B6 substrate characteristics, the cytochrome b_5 binding site and comparison with CYP2B1 and CYP2B4. *Xenobiotica* **29**, 361–393
16. Bridges, A., Gruenke, L., Chang, Y.T., Vakser, I.A., Loew, G., and Waskell, L. (1998) Identification of the binding site on cytochrome P450 2B4 for cytochrome b_5 and cytochrome P450 reductase. *J. Biol. Chem.* **273**, 17036–17049
17. Heinemann, F.S. and Ozols, J. (1983) The complete amino acid sequence of rabbit phenobarbital-induced liver microsomal cytochrome P-450. *J. Biol. Chem.* **258**, 4195–4201
18. Tarr, G.E., Black, S.D., Fujita, V.S., and Coon, M.J. (1983) Complete amino acid sequence and predicted membrane topology of phenobarbital-induced cytochrome P-450 (isozyme 2) from rabbit liver microsomes. *Proc. Natl. Acad. Sci. USA* **80**, 6552–6556
19. Vaz, A.D.N., McGinnity, D.F., and Coon, M.J. (1998) Epoxidation of olefins by cytochrome P450: evidence from site-specific mutagenesis for hydroperoxo-iron as an electrophilic oxidant. *Proc. Natl. Acad. Sci. USA* **95**, 3555–3560
20. Zhang, V. and Pernecky, S.J. (1999) Cumene hydroperoxide-supported demethylation reactions catalyzed by cytochrome P450 2B4 lacking the NH_2-terminal sequence. *Biochem. Biophys. Res. Commun.* **258**, 32–38
21. Papworth, C., Bauer, J.C., Braman, J., and Wright, D.A. (1996) Site-directed mutagenesis in one day with >80% efficiency. *Strategies* **8**, 3–4
22. Pernecky, S.J., Olken, N.M., Bestervelt, L.L., and Coon, M.J. (1995) Subcellular localisation, aggregation state, and catalytic activity of microsomal P450 cytochromes modified in the NH_2-terminal region and expressed in *Escherichia coli*. *Arch. Biochem. Biophys.* **318**, 446–456
23. Omura, T. and Sato, R. (1964) The carbon monoxide-binding pigment of liver microsomes. II. Solubilization, purification, and properties. *J. Biol. Chem.* **239**, 2379–2385
24. Laemmli, U.K. (1970) Cleavage of structural proteins during the assembly of the head of bacteriophage T4. *Nature* **227**, 680–685
25. Towbin, H., Staehelin, T., and Gordon, J. (1979) Electrophoretic transfer of proteins from polyacrylamide gels to nitrocellulose sheets: procedure and some applications. *Proc. Natl. Acad. Sci. USA* **76**, 4350–4354
26. Lowry, O.H., Rosebrough, N.J., Farr, A.L., and Randall, R.J. (1951) Protein measurement with the Folin phenol reagent. *J. Biol. Chem.* **193**, 265–275
27. Hlavica, P. and Hülsmann, S. (1979) Studies of the mechanism of hepatic microsomal *N*-oxide formation. *N*-oxidation of *N,N*-dimethylaniline by a reconstituted rabbit livermicrosomal cytochrome P-448 enzyme system. *Biochem. J.* **182**, 109–116
28. French, J.S., Guengerich, F.P., and Coon, M.J. (1980) Interactions of cytochrome P-450, NADPH-cytochrome P-450 reductase, phospholipid, and substrate in the reconstituted liver microsomal enzyme system. *J. Biol. Chem.* **255**, 4112–4119
29. Perella, F.W. (1988) EZ-FIT: a practical curve-fitting microcomputer program for the analysis of enzyme kinetic data on IBM-PC compatible computers. *Anal. Biochem.* **174**, 437–447
30. Horecker, B.L. and Kornberg, A. (1948) The extinction coefficients of the reduced band of pyridine nucleotides. *J. Biol. Chem.* **175**, 385–390
31. Hildebrandt, A.G., Roots, I., Tjoe, M., and Heinemeyer, G. (1978) Hydrogen peroxide in hepatic microsomes. *Methods Enzymol.* **52**, 342–350
32. Lewis, D.F.V. and Lake, B.G. (1997) Molecular modelling of mammalian CYP2B isoforms and their interaction with substrates, inhibitors and redox partners. *Xenobiotica* **27**, 443–478
33. Haugen, D.A. and Coon, M.J. (1976) Properties of electrophoretically homogenous phenobarbital-inducible and β-naphthoflavone-inducible forms of liver microsomal cytochrome P-450. *J. Biol. Chem.* **251**, 7929–7939
34. Jänig, G.R., Friedrich, J., Smettan, G., Bernhardt, R., Rustau, O., and Ruckpaul, K. (1985) Chemical modification of cytochrome P-450LM2 with N-acetylimidazole. Evidence for the functional involvement of tyrosyl residues. *Biomed. Biochim. Acta* **44**, 1071–1082
35. Hlavica, P. (1992) Analysis of the mode of interaction of NADPH-cytochrome P-450 reductase and cytochrome b_5 with cytochrome P-450LM2 (P-450IIB4) in *Cytochrome P-450: Biochemistry and Biophysics* (Archakov, A.I. and Bachmanova, G.I., eds.) pp.216–221, INCO-TNC, Joint Stock Company, Moscow
36. Hlavica, P., Lehnerer, M., and Eulitz, M. (1996) Histidine residues in rabbit liver microsomal cytochrome P-450 2B4 control electron transfer from NADPH-cytochrome P-450 reductase and cytochrome b_5. *Biochem. J.* **318**, 857–862
37. Shank-Retzlaff, M.L., Raner, G.M., Coon, M.J., and Sligar, S.G. (1998) Membrane topology of cytochrome P450 2B4 in Langmuir-Blodgett monolayers. *Arch. Biochem. Biophys.* **359**, 82–88
38. Lehnerer, M., Schulze, J., Pernecky, S.J., Lewis, D.F.V., Eulitz, M., and Hlavica, P. (1998) Influence of mutation of the amino-terminal signal anchor sequence of cytochrome P450 2B4 on the enzyme structure and electron transfer processes. *J. Biochem.* **124**, 396–403
39. Schulze, J., Lehnerer, M., Lewis, D.F.V., and Hlavica, P. (1998) Amino acid residue 250 has a functional role in the assembly of rabbit liver microsomal cytochrome P450 2B4. *Biochem. Mol. Biol. Int.* **44**, 1147–1155
40. Gotoh, O. and Fujii-Kuriyama, Y. (1989) Evolution, structure, and gene regulation of cytochrome P-450 in *Frontiers in Biotransformation* (Ruckpaul, K. and Rein, H., eds.) Vol. 1, pp. 195–243, Taylor & Francis, London
41. Hopfield, J.J. (1974) Electron transfer between biological molecules by thermally activated tunneling. *Proc. Natl. Acad. Sci. USA* **71**, 3640–3644
42. Vaz, A.D.N., Pernecky, S.J., Raner, G.M., and Coon, M.J. (1996) Peroxo-iron and oxenoid-iron species as alternative oxygenating agents in cytochrome P450-catalyzed reactions: switching by threonine-302 to alanine mutagenesis of cytochrome P450 2B4. *Proc. Natl. Acad. Sci. USA* **93**, 4644–4648
43. Nordblom, G.D. and Coon, M.J. (1977) Hydrogen peroxide formation and stoichiometry of hydroxylation reactions catalyzed by highly purified liver microsomal cytochrome P-450. *Arch. Biochem. Biophys.* **180**, 343–347
44. Bernhardt, R., Makower, A. Jänig, G.R., and Ruckpaul, K. (1984) Selective chemical modification of a functionally linked lysine in cytochrome P-450LM2. *Biochim. Biophys. Acta* **785**, 186–190